Available online at www.sciencedirect.com
SCIENCE DIRECT®
Journal of Solid State Chemistry 178 (2005) 897–901
JOURNAL OF SOLID STATE CHEMISTRY
www.elsevier.com/locate/jssc

Electrochemical properties and synthesis of $LiAl_{0.05}Mn_{1.95}O_{3.95}F_{0.05}$ by a solution-based gel method for lithium secondary battery

Ben-Lin He, Shu-Juan Bao, Yan-Yu Liang, Wen-Jia Zhou, Hua Li, Hu-Lin Li*

College of Chemistry and Chemical Engineering of Lanzhou University, Lanzhou 730000, PR China

Received 28 November 2004; received in revised form 17 January 2005; accepted 20 January 2005

Abstract

The cathode materials, $LiMn_2O_4$, $LiAl_{0.05}Mn_{1.95}O_4$ and $LiAl_{0.05}Mn_{1.95}O_{3.95}F_{0.05}$ were firstly prepared by a simple solution-based gel method using the mixture of acetate and ethanol as the chelating agent. The synthesized samples were investigated by X-ray diffraction, scanning electronic microscope and differential and thermal analysis. The as-prepared powders were used as positive materials for lithium-ion battery, whose discharge capacity and cycle voltammogram properties were examined. The results revealed that $LiAl_{0.05}Mn_{1.95}O_{3.95}F_{0.05}$ synthesized by the solution-based gel method had higher initial capacity than $LiAl_{0.05}Mn_{1.95}O_4$ and better capacity retention rate (92%) than that of $LiAl_{0.05}Mn_{1.95}O_4$ and $LiMn_2O_4$, which revealed that Al and F dual-doped $LiMn_2O_4$ could gain better electrochemical properties of $LiMn_2O_4$ than only the Al-doped $LiMn_2O_4$.

Keywords: Lithium-ion batteries; $LiMn_2O_4$; $LiAl_{0.05}Mn_{1.95}O_{3.95}F_{0.05}$; Dual-doped; Spinel

1. Introduction

Currently, $LiCoO_2$ is used as the main cathode material of lithium-ion batteries. However, because of the high cost and toxicity of cobalt, an intensive search for new cathode materials has been underway in recent years. One of the most attractive cathode materials is the spinel $LiMn_2O_4$ with a three-dimensional tunnel for the migration of lithium ions, which is a promising substitution for $LiCoO_2$, due to its advantages such as lower cost, higher abundance of Mn in the earth, good safety and nontoxicity. In spite of these advantages, $LiMn_2O_4$ has the problem of severe capacity fading during charge and discharge cycles, which makes it unsuitable for commercial performances. This problem has been discussed based on the following factors: manganese dissolution [1,2], electrolyte decomposition at high potentials [3,4], Jahn–Teller distortion at the deeply discharged state [5], and lattice instability [6]. Of the above factors, dissolution of manganese into the electrolyte during cycling is believed to be the main one. Several researchers have studied that reducing the amount of the Mn^{3+} ion in structure may help in improve the cycling performance of Mn spinel [7–9]. One approach is the substitution of Mn by other metal cations such as Al, Ni, Cr, Co, etc. [10–13] which can make the structure of spinel $LiMn_2O_4$ more stable. Although such substitutions often result in enhanced stability of the spinel, the first discharge capacity is found to be considerably lower than that of the parent compound. The reduction in capacity is mainly due to the fact that the substituent ions do not contribute to the charge capacity. Recently, Amatucci et al. [14] and Palacin et al. [15] have reported that the introduction of anion substitution in the form of spinel oxyfluorides can reduce the Mn oxidation state and then increased the specific capacity. Since the aluminum is abundant, less expensive, and lighter than the transition metal group, Al-substituted manganese oxide is expected to be a

*Corresponding author. Fax: +86 931 891 2582.
E-mail address: lihl@lzu.edu.cn (H.-L. Li).

0022-4596/$ - see front matter © 2005 Elsevier Inc. All rights reserved.
doi:10.1016/j.jssc.2005.01.015

cathode material with lower cost than $LiMn_2O_4$ [16]. Accordingly, we have synthesized Al, F dual-doped substituted $LiMn_2O_4$ in this work.

Spinel $LiMn_2O_4$ powders are typically synthesized using a conventional solid-state reaction method that requires long and repeated heat-treatment processes. This method also has many disadvantages, such as inhomogeneity, irregular morphology, large particle size and broad particle size distribution and poor control of stoichiometry. Such disadvantages are expected to be solved by employing soft chemistry methods, such as sol–gel synthesis [17], precipitation [18], and the Pechini process [19]. That is, all the components can be distributed homogeneously on the atomic scale, so that the calcinations process would be able to be reduced and the particle size can be controlled. Here, an attempt has been made to stabilize the $LiMn_2O_4$ spinel structure by a solution-based gel method that employs the mixture of acetate and ethanol as the chelating agent with Al, F as the dopants. This soft chemistry technique is simpler and more economical compared with the traditional sol–gel method, What's more, $LiMn_2O_4$ cathode materials synthesized by the soft chemistry technique has many advantages such as better homogeneity, less heating time, regular morphology, less impurities, large surface area, and good control of stoichiometry.

In this paper, we prepared Al and F dual-doped $LiMn_2O_4$ by a solution-based gel method. Their physical properties have been studied by X-ray diffraction (XRD), scanning electronic microscope (SEM), differential and thermal analysis (DTA/TG). The effect of partial Al^{3+} substitution for Mn^{3+} and partial F^- substitution for O^{2-} in $LiMn_2O_4$ positive electrodes on its electrochemical properties in Li cells has been investigated in detail.

2. Experimental

The samples of substituted spinel compound $LiAl_xMn_{2-x}O_{4-z}F_z$ were prepared by a solution-based gel method. Stoichiometric amounts of lithium acetate [$Li(CH_3COO)\cdot 4H_2O$], manganese acetate [$Mn(CH_3COO)_2\cdot 4H_2O$], aluminum nitrate [$Al(NO_3)_3\cdot 9H_2O$] and lithium fluoride [LiF] were dissolved in distilled water into which the mixture of acetate and ethanol was added dropwise under continuous stirring. Thereafter, ammonium hydroxide [$NH_3\cdot H_2O$] was added slowly to the solution to control the pH at ~8. The prepared solution was then heated at 70~80 °C to evaporate the water until a transparent gel was obtained. The resulting gel precursor was decomposed at 450 °C for 5 h in air to remove the organic contents. Then, the resulting precursor was ground to fine powders and calcined at 800 °C in air for 10 h to obtain the final spinel product.

Powder XRD using D/max-2400 Rigaku (Japan) with Cu$K\alpha$ monochromated radiation was performed to identify the crystalline phase of the samples. XRD data were collected in the 2θ ranges from 10° to 80°.

Differential thermal analysis (DTA) and thermogravimetery (TG) measurements were performed in air from room temperature to 800 °C with a Dupont 1090B thermal analysis system under a scanning rate of 10 °C/min. a-Al_2O_3 was used as the reference material and the platinum crucible as the vessel for samples. The weight of the samples was ca. 20 mg.

The positive electrodes were fabricated by intimately mixing the active material (80%), acetylene black (15%) and binder (5 wt% polyvinylidene fluoride, PVDF, dissolved in *N*-methyl-2-pyrrolidone, NMP) were mixed to form a slurry. The mixed slurry was coated onto an aluminum current collector. The electrodes were dried under vacuum at 100 °C overnight and then punched and weighed. The cells were assembled in a glove box under a dry argon atmosphere. The complete cell compromises a cathode, a celgard (2400) as the separator and an Li-foil anode. 1 M $LiPF_6$ (battery grade) dissolved in a mixture of ethylene carbonate (EC, battery grade) and dimethyl carbonate (DMC, battery grade) (1:1 by volume) was used as the electrolyte. Charge–discharge performance of the cell was characterized galvanostatically on Land CT2001A (Wuhan, China) at C/3 charge–discharge rate between 3.0 and 4.4 V (vs. Li/Li^+). Cyclic voltammograms (CVs) were measured on an electrochemical workstation (CHI660A) at a scan rate of 0.1 mV/s between 3.2 and 4.7 V (vs. Li/Li^+).

3. Results and discussion

Fig. 1 shows the TG–DTA curves for the thermal decomposition of the precursor $LiAl_{0.05}Mn_{1.95}O_{3.95}F_{0.05}$. Weight loss occurs in four temperature regions: 20–120, 120–250, 250–450, 450–800 °C. The little weight loss of the first region may be attributed to the superficial water loss due to the hygroscopic nature of the precursor complex. In the second region, the DTA curve shows two endothermic peaks at 180 and 230 °C, which are attributed to the loss of water of chemical bond water in the sample. In the third region, the two exothermic peaks observed at 320 and 390 °C are accompanied by noticeable weight lose in the TG curve. It is due to the decomposition of the inorganic and the organic constituents of the precursor followed by crystallization of $LiMn_2O_4$ phase. In the last region, the TG curve becomes flat and no sharp peaks can be observed in the DTA curve, indicating that no phase transformation occurs, and that any further heating only makes the structure of samples more crystalline.

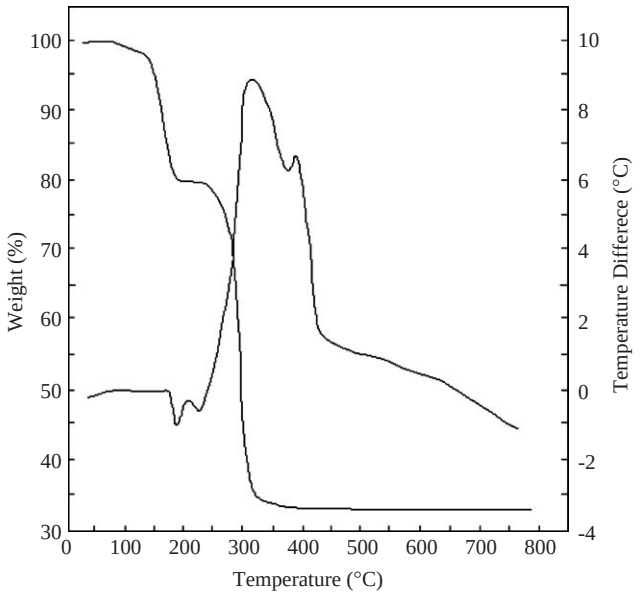

Fig. 1. The TG–DTA curves for the thermal decomposition of the precursor $LiAl_{0.05}Mn_{1.95}O_{3.95}F_{0.05}$.

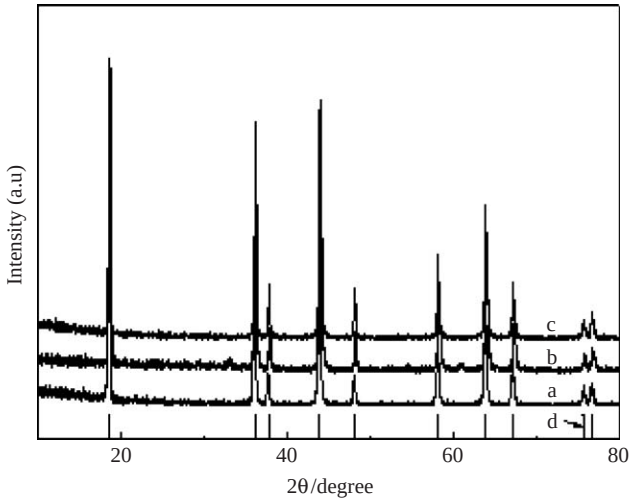

Fig. 2. The typical powder XRD patterns of (a) $LiMn_2O_4$ (b) $LiAl_{0.05}Mn_{1.95}O_4$ (c) $LiAl_{0.05}Mn_{1.95}O_{3.95}F_{0.05}$ (d) vertical bars of the expected X-ray pattern for the $LiMn_2O_4$ spinel.

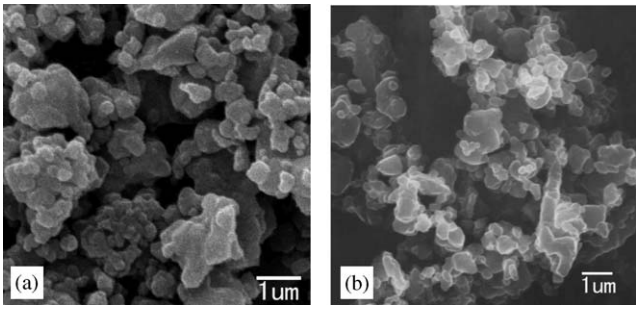

Fig. 3. Typical SEM photographs of (a) $LiAl_{0.05}Mn_{1.95}O_4$ and (b) $LiAl_{0.05}Mn_{1.95}O_{3.95}F_{0.05}$.

The typical powder XRD patterns of $LiAl_xMn_{2-x}O_{4-z}F_z$ (*a*, *b*, *c*) and the vertical bars of the expected X-ray pattern for the $LiMn_2O_4$ spinel (d) are shown in Fig. 2. All samples were identified as a pure spinel phase with a space group *Fd*3*m* where lithium ions occupy the tetrahedral (8*a*) sites, Mn^{3+}, Mn^{4+} and Al^{3+} ions reside at the octahedral (16*d*) sites [13]. No additional peaks for other second phases such as Al_2O_3, $LiAlO_2$ or LiF were observed. We calculated the lattice parameters of the samples from the diffraction data through the least square program method and found that $LiAl_{0.05}Mn_{1.95}O_4$ has a smaller lattice parameters (8.212 ± 0.004 Å) value compared with $LiMn_2O_4$ (8.245 ± 0.004 Å). In fact, substitution of manganese by aluminum should result in shrinkage of the unit cell volume. This is because aluminum ions have smaller ionic radii than manganese ions: Al^{3+} (0.53 Å), Mn^{3+} (0.66 Å), Mn^{4+} (0.60 Å) [14]. The decrease in cell volume should increase the stability of the structure during insertion and deinsertion of lithium [20]. However, the $LiAl_{0.05}Mn_{1.95}O_{3.95}F_{0.05}$ has a little larger lattice parameter (8.223 ± 0.004 Å) than the $LiAl_{0.05}Mn_{1.95}O_4$, which is due to that monovalent fluorine substitutes for divalent oxygen reduces Mn^{4+} to Mn^{3+} and thus increase the quantity of the larger trivalent manganese Mn^{3+} (0.66 Å). The increase of Mn^{3+} will slightly increase the unit cell volume of $LiAl_{0.05}Mn_{1.95}O_{3.95}F_{0.05}$ compared to that of $LiAl_{0.05}Mn_{1.95}O_4$ and elevated the initial specific capacity.

Typical SEM photographs of $LiAl_{0.05}Mn_{1.95}O_4$ and $LiAl_{0.05}Mn_{1.95}O_{3.95}F_{0.05}$ prepared by the solution-based gel method are shown in Fig. 3a and b, respectively. All of the as-prepared powders had the uniform, nearly cubic structure morphology with narrow size distribution. Compared with $LiAl_{0.05}Mn_{1.95}O_4$, the Al and F dual-doped sample $LiAl_{0.05}Mn_{1.95}O_{3.95}F_{0.05}$ showed a slightly smaller particle size value and a more regular morphology structure because the addition of precursor LiF as a flux in crystal growth can lead to a better controlling morphology and particle size of the spinel. In addition, the particles of $LiAl_{0.05}Mn_{1.95}O_{3.95}F_{0.05}$ are distributed more uniformly than that of $LiAl_{0.05}Mn_{1.95}O_4$. The aforementioned features of $LiAl_{0.05}Mn_{1.95}O_{3.95}F_{0.05}$ are very desirable for being employed as the electrode material to improve the electrochemical properties of spinel $LiMn_2O_4$ cathode materials for lithium rechargeable batteries.

Fig. 4 shows the first charge–discharge curves of $Li/LiMn_2O_4$, $Li/LiAl_{0.05}Mn_{1.95}O_4$ and $Li/LiAl_{0.05}Mn_{1.95}O_{3.95}F_{0.05}$ cells. It can be seen obviously that the charge/discharge curves of all the samples had two voltage plateaus at approximately 4.0 and 4.1 V, which indicated a remarkable characteristic of a well-defined

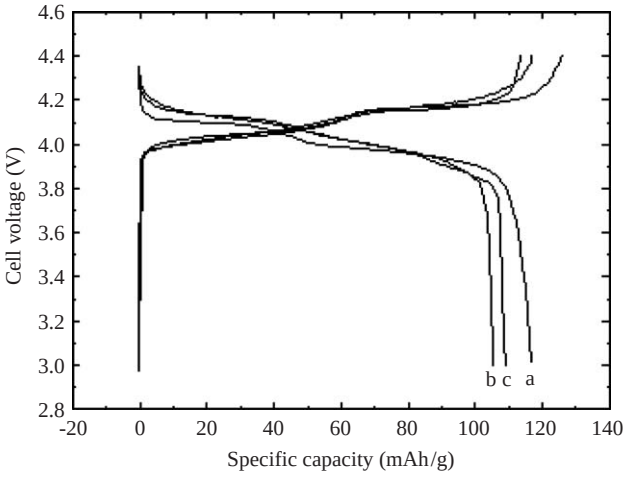

Fig. 4. Charge–discharge curves of cells (a) $Li/LiMn_2O_4$, (b) $Li/LiAl_{0.05}Mn_{1.95}O_4$ and (c) $Li/LiAl_{0.05}Mn_{1.95}O_{3.95}F_{0.05}$ at first cycle.

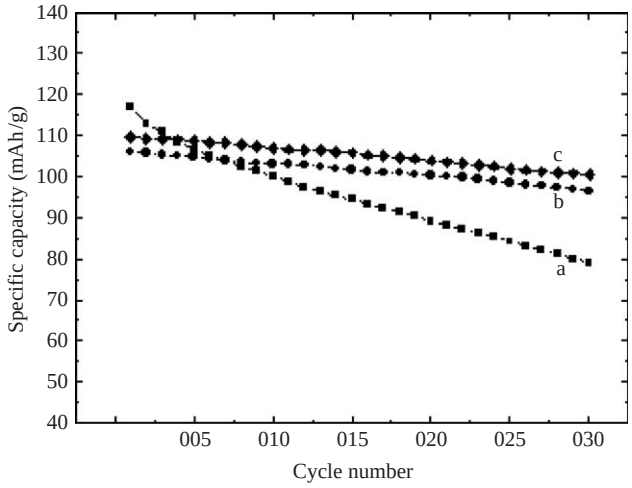

Fig. 5. Cycle performance of cells (a) $Li/LiMn_2O_4$, (b) $Li/LiAl_{0.05}Mn_{1.95}O_4$ and (c) $Li/LiAl_{0.05}Mn_{1.95}O_{3.95}F_{0.05}$.

$LiMn_2O_4$ spinel. The two voltage plateaus indicate that the insertion and extraction of lithium ions occur in two stages [21]. The first voltage plateau at about 4.0 V is attributed to the removal of lithium ions from half of the tetrahedral sites in which Li–Li interactions occur. The second voltage plateau observed at about 4.1 V is due to the removal of lithium ions from the other tetrahedral sites in which lithium ions do not have Li–Li interactions.

The initial capacity of $LiAl_{0.05}Mn_{1.95}O_{3.95}F_{0.05}$ and $LiAl_{0.05}Mn_{1.95}O_4$ is lower than that of pure $LiMn_2O_4$. The initial capacity of $LiMn_2O_4$ and $LiAl_{0.05}Mn_{1.95}O_4$ is 117 and 106 mAh/g, respectively. This decrease of initial capacity is due to the decreasing amount of Mn^{3+} ions in Al substituted spinel phase. In fact, only the Mn^{3+} contributes to charge/discharge capacity during the intercalation–deintercalation of Li^+ in $LiMn_2O_4$. However, the initial discharge capacity of $LiAl_{0.05}Mn_{1.95}O_{3.95}F_{0.05}$ (110 mA h/g) is higher than that of $LiAl_{0.05}Mn_{1.95}O_4$ because of the reduction of some Mn^{4+} to Mn^{3+} caused by monovalent fluorine substituted for divalent oxygen, which increases the amount of Mn^{3+} content available for redox (thereby increasing the specific capacity). These results are in agreement with the XRD analysis above.

The cycleability curves for pure $LiMn_2O_4$, $LiAl_{0.05}Mn_{1.95}O_4$ and $LiAl_{0.05}Mn_{1.95}O_{3.95}F_{0.05}$ are shown in Fig. 5. It is obviously found that the cyclibility of the Al-doped $LiAl_{0.05}Mn_{1.95}O_4$ and Al, F dual-doped $LiAl_{0.05}Mn_{1.95}O_{3.95}F_{0.05}$ was significantly improved. Although the pure $LiMn_2O_4$ had the highest initial discharge capacity, its capacity loss was 32% of the initial value after 30 cycles between 3.0 and 4.4 V at C/3 charge–discharge rate. However, the capacity loss of $LiAl_{0.05}Mn_{1.95}O_{3.95}F_{0.05}$ was only 8% of its initial capacity at the 30th cycle. Moreover, the Al, F dual-doped spinel showed slightly better cycle performance compared with the Al-doped spinel. Thus, the simultaneously cation- and anion-sites substitution of $LiMn_2O_4$ with Al and F improved the cycling performance of spinel $LiMn_2O_4$ more than cation-only substitution of $LiMn_2O_4$ with Al.

Because substitution of manganese by aluminum decreases the unit cell volume and the decrease of Mn^{3+} concentration reduces the Jahn–Teller distortion and also stabilizes the structure integrity of the active, improved electrochemical stability of Al-doped $LiMn_2O_4$ electrode is obtained. The strength of Al–O bond is another reason for the enhanced cyclibility of Al-doped $LiMn_2O_4$ electrode because the bonding energy of Al–O (512 kJ/mol) is stronger than that of Mn–O (402 kJ/mol) [22]. This prevents the structural disintegration of the material. The $LiAl_{0.05}Mn_{1.95}O_{3.95}F_{0.05}$ compound has a more stable cycle life than $LiAl_{0.05}Mn_{1.95}O_4$ because the dual doping of Al and F increases the binding energy in the octahedral MO_6 sites. Therefore, the entire spinel structure becomes more stable despite a slightly larger unit cell volume.

The cycle voltammogram properties of the cells $LiMn_2O_4$ and $LiAl_{0.05}Mn_{1.95}O_{3.95}F_{0.05}$ after 5 and 30 cycles were tested. Cyclic voltammograms (sweep rate: 0.1 mV/s) in the potential region of 3.2–4.7 V are presented in Fig. 6a and b, respectively. The cyclic voltammograms show two symmetrical couples of redox peaks at around 4.0 and 4.1 V, which is associated with the processes observed in the charge–discharge test and also indicates that the intercalation and deintercalation of lithium-ion in the spinel are reversible. After 30 cycles, the shape of the cyclic voltammograms became poor for all samples, especially pure $LiMn_2O_4$. Compared with pure $LiMn_2O_4$, the redox peaks of $LiAl_{0.05}Mn_{1.95}O_{3.95}F_{0.05}$ electrode after 5 and 30

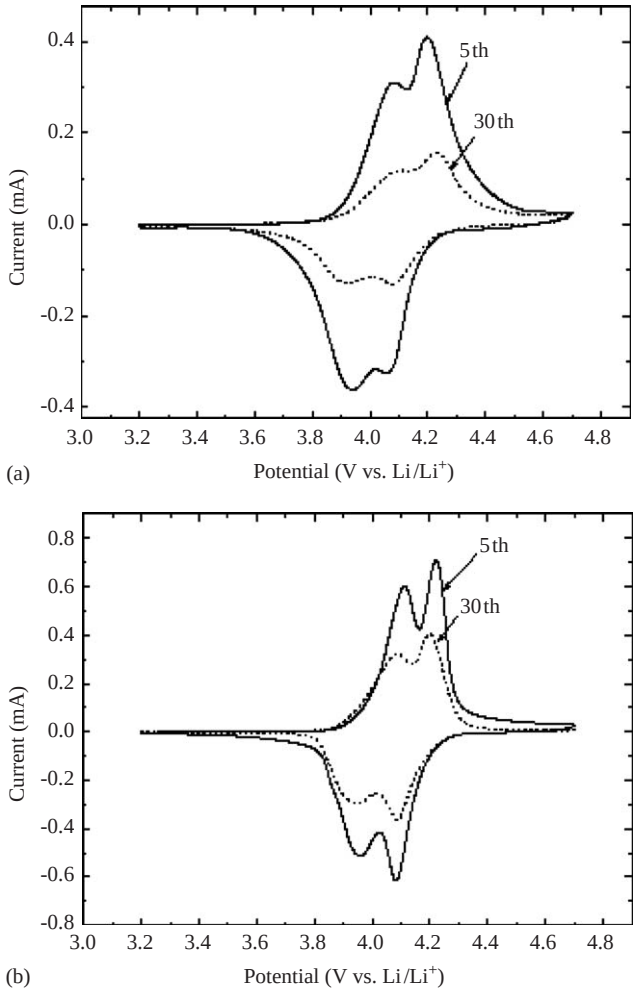

Fig. 6. Cyclic voltammograms of cells containing (a) $LiMn_2O_4$ and (b) $LiAl_{0.05}Mn_{1.95}O_{3.95}F_{0.05}$ after 5 and 30 cycles.

cycles are sharp and show well-defined splitting, which indicates that the Al, F dual-doped $LiAl_{0.05}Mn_{1.95}O_{3.95}F_{0.05}$ powders are more crystalline than pure $LiMn_2O_4$ and also explains that the cycle performance of $LiAl_{0.05}Mn_{1.95}O_{3.95}F_{0.05}$ is better than $LiMn_2O_4$. The same results are obtained in the cycleability measurements.

4. Conclusion

The $LiAl_xMn_{2-x}O_{4-z}F_z$ cathode materials were successfully prepared by a solution-based gel method using the mixture of acetate and ethanol as the chelating agent. All of the as-prepared powders were well crystallized to a single spinel structure with *Fd3m* space group. The SEM test revealed that the $LiAl_{0.05}Mn_{1.95}O_{3.95}F_{0.05}$ powder had a slightly smaller particle size value and a more regular morphology than the $LiAl_{0.05}Mn_{1.95}O_4$. Electrochemical measurements of the as-prepared samples as cathode for Li ion batteries have shown that the $LiAl_{0.05}Mn_{1.95}O_{3.95}F_{0.05}$ has a more stable cycle performance than $LiAl_{0.05}Mn_{1.95}O_4$ and $LiMn_2O_4$. The capacity deterioration of $LiAl_{0.05}Mn_{1.95}O_{3.95}F_{0.05}$ was only 8% of its initial capacity while the capacity loss of pure $LiMn_2O_4$ was 32%, which revealed that the simultaneous substitution of cation- and anion-sites of $LiMn_2O_4$ with Al and F was a very effective method for improving the performance of spinel $LiMn_2O_4$ for lithium rechargeable batteries.

Acknowledgments

The authors are thankful for the support provided by National Nature Science Foundation of China (No. 60471014).

References

[1] A. Blyr, C. Sigala, G.G. Amatucci, D. Guyomard, Y. Chabre, J.M. Tarascon, J. Electrochem. Soc. 145 (1998) 194–199.
[2] X. Sun, H.S. Lee, X.Q. Yang, J. McBreen, Electrochem. Solid-State Lett. 4 (2001) A184–A186.
[3] G.G. Amatucci, C.N. Schmutz, A. Blyr, C. Sigala, A.S. Gozdz, D. Larcher, J.M. Tarascon, J. Power Sources 69 (1997) 11–25.
[4] R.J. Gummow, A. de Knok, M.M. Thackeray, Solid State Ionics 69 (1994) 59–67.
[5] M.M. Thackeray, Y. Shao-Horm, A.J. Kahainan, K.D. Kepler, E. Skinner, J.T. Vaughey, H.S.A. Hackney, Electrochem. Solid-State Lett. 1 (1998) 7–9.
[6] A. Yamada, J. Solid State Chem. 122 (1996) 160–165.
[7] D. Guyomard, J.M. Tarascon, Solid State Ionics 69 (1994) 222–237.
[8] X. Qiu, X. Sun, W. Shen, N. Chen, Solid State Ionics 93 (1997) 335–339.
[9] Y. –K. Sun, Solid State Ionics 100 (1997) 115–125.
[10] A.D. Roberston, S.H. Lu, W.F. Averill, W.F. Howard Jr., J. Electrochem. Soc. 144 (1997) 3500–3504.
[11] A.D. Roberston, S.H. Lu, W.F. Howard Jr., J. Electrochem. Soc. 144 (1997) 3505–3512.
[12] K. Amine, H. Tukamoto, H. Yasada, Y. Fujita, J. Electrochem. Soc. 143 (1996) 1607–1612.
[13] L. Guohua, H. Ikuta, T. Uchida, M. Wakihara, J. Electrochem. Soc. 143 (1996) 178–182.
[14] G.G. Amatucci, N. Pereira, T. Zhang, I. Plitz, J.M. Tarascon, J. Power Sources 81-82 (1999) 39–43.
[15] M.R. Palacin, F.L. Cras, L. Seguin, M. Anne, Y. Chabre, J.M. Tarascon, G. Amatucci, G. Vaughan, P. Strobel, J. Solid State Chem. 144 (1999) 361–371.
[16] Seung-Taek. Myung, Shinichi. Komaba, Naoaki. Kumagai, J. Electrochem. Soc. 148 (2001) A482–A489.
[17] Y.-K. Sun, C.S. Yoon, C.K. Kim, S.G. Youn, Y.-S. Lee, M. Yoshio, I.-H. Oh, J. Mater. Chem. 11 (2001) 2519–2522.
[18] P. Barboux, J.M. Tarascon, F.K. Shokoohi, J. Solid State Chem. 94 (1991) 185–196.
[19] G.X. Wang, D.H. Bradhurst, H.K. Liu, S.X. Dou, Solid State Ionics 120 (1999) 95–101.
[20] E. Iwata, K. Takahashi, T. Maeda, T. Mouri, J. Power Sources 81–82 (1999) 430–433.
[21] Y. Xia, M. Yoshio, J. Electrochem. Soc. 143 (1996) 825–833.
[22] J.A. Dean, Lange's Handbook of Chemistry, fourth ed, McGraw-Hill, Inc., New York, 1992.